



The positivity-preserving finite volume scheme with fixed stencils for radiation diffusion problems on general polyhedral meshes

Zhi-Ming Gao

Joint work with Dr. Di Yang

ZABABA KHIN SCIENTIFIC TALKS 2023



铸国防基石 做民族脊梁

Outline

- 1 Motivation**
- 2 PPFV scheme for steady diffusion problem**
- 3 PPFV scheme for three temperature model**
- 4 Numerical examples**

Outline

1 Motivation

2 PPFV scheme for steady diffusion problem

3 PPFV scheme for three temperature model

4 Numerical examples

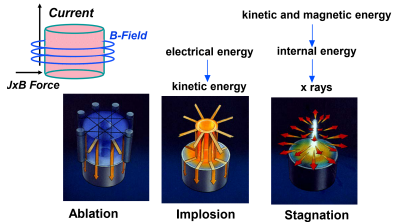
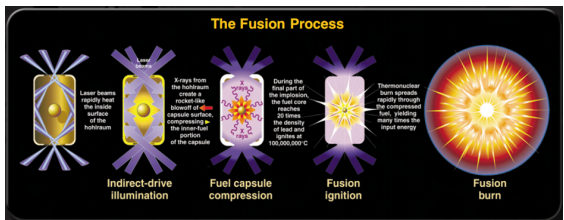
A three temperature plasma model in ICF

Development of new methods is mainly driven by needs of large scale multiphysics simulation, for instance a three temperature plasma model in the fields of inertial confinement fusion

$$\frac{\partial E_e}{\partial t} - \nabla \cdot (\lambda'_e \nabla T_e) = c\sigma_P (E_r - aT_e^4) + c\kappa (T_i - T_e) + Q_e,$$

$$\frac{\partial E_i}{\partial t} - \nabla \cdot (\lambda'_i \nabla T_i) = c\kappa (T_e - T_i) + Q_i,$$

$$\frac{\partial E_r}{\partial t} - \nabla \cdot (\lambda_r \nabla E_r) = c\sigma_P (aT_e^4 - E_r) + Q_r.$$



A three temperature plasma model in ICF

The three energies E_e , E_i and E_r can not be negative, and a conservative postprocessing is not a best choice. It adds additional complexity that can be used to build a better discretization method.

$$\begin{aligned}\frac{\partial E_e}{\partial t} - \nabla \cdot (\lambda'_e \nabla T_e) &= c\sigma_P (E_r - aT_e^4) + c\kappa (T_i - T_e) + Q_e, \\ \frac{\partial E_i}{\partial t} - \nabla \cdot (\lambda'_i \nabla T_i) &= c\kappa (T_e - T_i) + Q_i, \\ \frac{\partial E_r}{\partial t} - \nabla \cdot (\lambda_r \nabla E_r) &= c\sigma_P (aT_e^4 - E_r) + Q_r.\end{aligned}$$

The goal of this talk: construct a positivity-preserving finite volume scheme (PPFV) for the three temperature model !

Positivity-preserving property

$$\frac{\partial E_e}{\partial t} - \nabla \cdot (\lambda'_e \nabla T_e) = S_e(T) + Q_e$$

$$\frac{\partial E_i}{\partial t} - \nabla \cdot (\lambda'_i \nabla T_i) = S_i(T) + Q_i$$

$$\frac{\partial E_r}{\partial t} - \nabla \cdot (\lambda_r \nabla E_r) = S_r(T) + Q_r$$

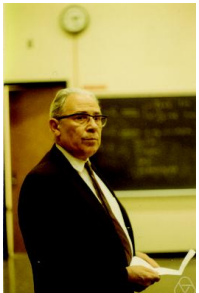
For simplicity

$$-\nabla \cdot (\Lambda \nabla u) = f$$

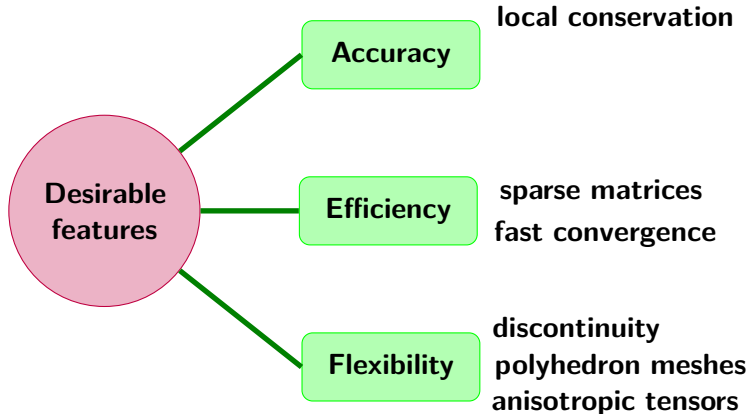
Positivity-preserving property

Let $u \in C^2(\Omega) \cap C^0(\bar{\Omega})$ satisfy that $f \geq 0$ in Ω and $u \geq 0$ on $\partial\Omega$ under the assumption that Λ should be locally uniformly positive definite in Ω . Then $u \geq 0$ in Ω .

From the weak maximum principle, this property is immediate to derive.



Why nonlinear finite volume scheme?

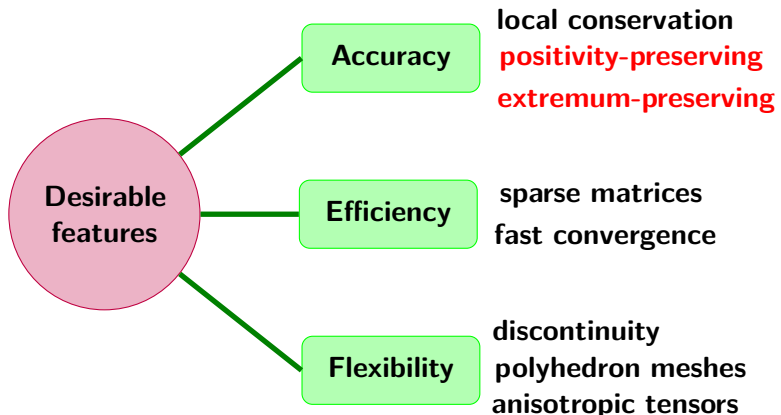


Linear schemes

- | | |
|--------|-----|
| ● FEM | VEM |
| ● MFD | MFV |
| ● MPFA | HFV |
| ● LPFV | NPS |

Positivity-preserving property: impose some restrictions on mesh topology and anisotropy of diffusion tensor Λ !

Why nonlinear finite volume scheme?



Linear schemes

- | | |
|--------|------|
| ● FEM | VEIM |
| ● MFD | MFV |
| ● MPFA | HFV |
| ● LPFV | NPS |

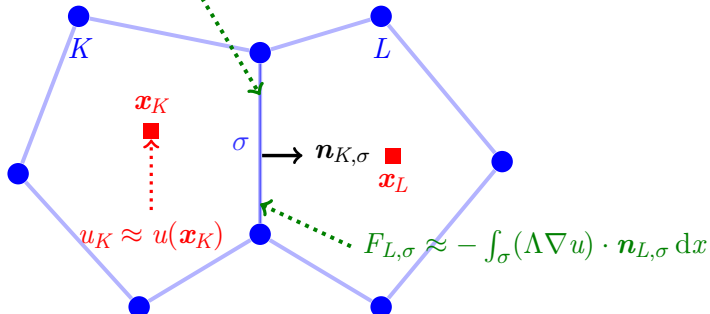
Nonlinear schemes

- NLTPFA
- NMPFA
- Postprocessing

Expensive to solve the nonlinear system $A(U)U = F(U)$ but may be very nice for Newton type methods in a multiphysics simulations such as a 3T plasma model !

Principle of finite volume methods

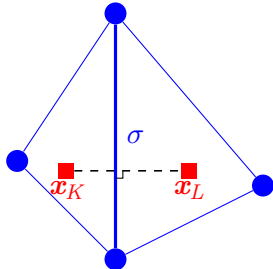
$$F_{K,\sigma} \approx - \int_{\sigma} (\Lambda \nabla u) \cdot \mathbf{n}_{K,\sigma} \, dx$$



(Flux balance) $\forall K : \sum_{\sigma \in \mathcal{E}_K} F_{K,\sigma} = |K| f_K.$

(Flux conservativity) $\forall \sigma = K|L : F_{K,\sigma} + F_{L,\sigma} = 0.$

PPFV scheme with a nonlinear TPFA



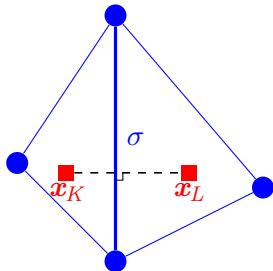
$\forall \sigma = K|L, (\mathbf{x}_K \mathbf{x}_L) \perp \sigma$

Two-Point Flux Approximation

- Assume that $(\mathbf{x}_K \mathbf{x}_L) \perp \sigma$ and $\Lambda = \text{Id}$, the classical TPFA is

$$F_{K,\sigma} = \int_{\sigma} -\Lambda \nabla u \cdot \mathbf{n}_{K,\sigma} = |\sigma| \frac{u(\mathbf{x}_K) - u(\mathbf{x}_L)}{\text{d}(\mathbf{x}_K, \mathbf{x}_L)}$$

PPFV scheme with a nonlinear TPFA



Two-Point Flux Approximation

- Assume that $(x_K x_L) \perp \sigma$ and $\Lambda = \text{Id}$, the classical TPFA is

$$F_{K,\sigma} = \int_{\sigma} -\Lambda \nabla u \cdot n_{K,\sigma} = |\sigma| \frac{u(x_K) - u(x_L)}{d(x_K, x_L)}$$

$$\forall \sigma = K|L, (x_K x_L) \perp \sigma$$

- TPFA is linear and monotone, but inaccurate for arbitrary meshes.
- Pioneer work (C Le Potier, 2005):** a nonlinear TPFA on triangle grids

$$F_{K,\sigma} = \alpha_{K,\sigma}(u)u_K - \alpha_{L,\sigma}(u)u_L \text{ with } \alpha_{K,\sigma} > 0 \text{ and } \alpha_{L,\sigma} > 0.$$

- We need interpolation method for auxiliary cell-vertex unknowns.

PPFV scheme with a nonlinear TPFA

Interpolation-based PPFV scheme

- general meshes or general diffusion tensors:(Lipnikov et.al. 07)(Kapyrin, 07)(Yuan & Sheng, 08,12)(Wang,Hang,Yuan, 2018)(Xie,et.al,2018)(Peng, Yang, Gao, 2021,2022)
- Interpolation method for auxiliary unknowns affects the accuracy.

Interpolation-free PPFV schemes

- Refs. (Lipnikov et.al., 09) (Danilov & Vassilevski, 09) (Lipnikov et.al., 12)
- need to know the location of discontinuity beforehand

VEM-based PPFV schemes

- use VEM for auxiliary unknowns (Sheng, Yang, Gao,2022)

Our goal in this talk

Design the interpolation-based PPFV scheme with approximately 2nd-order accuracy for three temperature radiation diffusion problems on general polyhedral meshes.

Outline

- 1 Motivation
- 2 PPFV scheme for steady diffusion problem
- 3 PPFV scheme for three temperature model
- 4 Numerical examples

The framework for the cell-centered FVM

1 Construct the one-sided flux

$$F_{K,\sigma} = \sum_{i=1}^{n_K} \alpha_{K,\sigma,i} (u_K - u_{K,i})$$

2 Define the unique flux

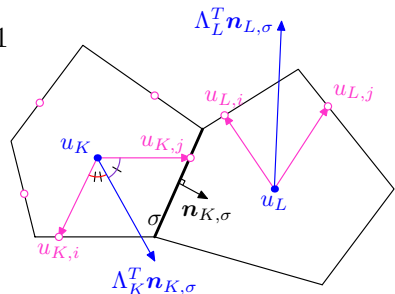
$$\tilde{F}_{K,\sigma} = \mu_{K,\sigma} F_{K,\sigma} - \mu_{L,\sigma} F_{L,\sigma}, \quad \mu_{K,\sigma} + \mu_{L,\sigma} = 1$$

3 The interpolation method for auxiliary unknowns

$$u_{K,i} = \sum_{L \in \mathcal{T}_{K,i}} \omega_{K,i}^L u_L$$

4 The final FV equation

Solve $\{u_K, K \in \mathcal{T}\}$ s.t. $\sum_{\sigma \in \mathcal{E}_K} \tilde{F}_{K,\sigma} = |K|f_K, \quad \forall K \in \mathcal{T}.$

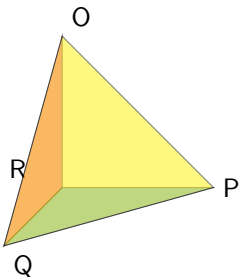


Step 1: construction of one-sided flux

- Discretization of the flux

$$F_{K,\sigma} = - \int_{\sigma} (\Lambda_K \nabla u) \cdot n_{K,\sigma} ds \simeq -|\sigma| (\Lambda_K \nabla u) \cdot \mathbf{n}_{K,\sigma} = -|\sigma| \Lambda_K^\top \mathbf{n}_{K,\sigma} \cdot \nabla u.$$

- Discretization of gradient



Let T_{OPQR} be a tetrahedron composed of vertex O, P, Q, R , and $\det(\mathbb{X}) > 0$:

$$\mathbb{X} = \begin{pmatrix} \overrightarrow{OP}^\top \\ \overrightarrow{OQ}^\top \\ \overrightarrow{OR}^\top \end{pmatrix} = \begin{pmatrix} x_P - x_O & y_P - y_O & z_P - z_O \\ x_Q - x_O & y_Q - y_O & z_Q - z_O \\ x_R - x_O & y_R - y_O & z_R - z_O \end{pmatrix}.$$

Hence for the function u defined on the tetrahedron T_{OPQR} , we have

$$\nabla u \simeq \frac{1}{6 V_{T_{OPQR}}} \left[(u_P - u_O)(\overrightarrow{OQ} \times \overrightarrow{OR}) + (u_Q - u_O)(\overrightarrow{OR} \times \overrightarrow{OP}) + (u_R - u_O)(\overrightarrow{OP} \times \overrightarrow{OQ}) \right].$$

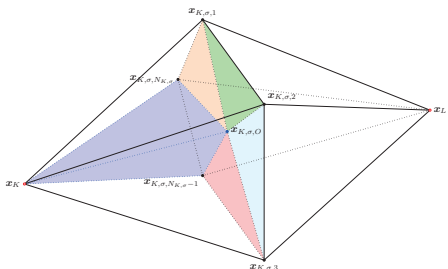
Step 1: construction of one-sided flux

- The linearity-preserving one-sided flux

$$F_{K,\sigma} = \sum_{i=1}^{N_{K,\sigma}} a_{K,\sigma,i} (\textcolor{red}{u_K} - u_{K,\sigma,i}), \quad K \in \mathcal{T}.$$

If K is a star-shaped polyhedron w.r.t. x_K , then it can be proved that

$$\sum_{i=1}^{N_{K,\sigma}} a_{K,\sigma,i} > 0, \quad \sigma \in \mathcal{E}_K.$$



Gradient on tetrahedron $x_K x_{K,\sigma,O} x_{K,\sigma,i} x_{K,\sigma,i+1}$

$$(\nabla u)|_{K,\sigma,i} \simeq \alpha_{K,\sigma,i}^1 (\textcolor{teal}{u}_{K,\sigma,O} - \textcolor{red}{u}_K) + \alpha_{K,\sigma,i}^2 (\textcolor{blue}{u}_{K,\sigma,i} - \textcolor{red}{u}_K) + \alpha_{K,\sigma,i}^3 (\textcolor{blue}{u}_{K,\sigma,i+1} - \textcolor{red}{u}_K).$$

Step 2: construction of the final flux

$$\tilde{F}_{K,\sigma} = \left(\mu_{K,\sigma} \sum_{i=1}^{n_K} \alpha_{K,\sigma,i} \right) \textcolor{red}{u_K} - \left(\mu_{L,\sigma} \sum_{i=1}^{n_L} \alpha_{L,\sigma,i} \right) \textcolor{red}{u_L} + \textcolor{blue}{B_\sigma}$$

$(\mu_{L,\sigma} a_{L,\sigma} - \mu_{K,\sigma} a_{K,\sigma})$



Step 2: construction of the final flux

$$\tilde{F}_{K,\sigma} = \left(\frac{a_{K,\sigma}}{a_{K,\sigma} + a_{L,\sigma}} \mu_{K,\sigma} \sum_{i=1}^{n_K} \alpha_{K,\sigma,i} \right) \textcolor{red}{u_K} - \left(\mu_{L,\sigma} \sum_{i=1}^{n_L} \alpha_{L,\sigma,i} \right) \textcolor{red}{u_L} + B_\sigma$$

($\mu_{L,\sigma} a_{L,\sigma} - \mu_{K,\sigma} a_{K,\sigma}$)

↓

Classical NLTPFA [C. Le Potier, CRAS'05]

↑

$$\tilde{F}_{K,\sigma} = A_{K,\sigma}(u) \textcolor{red}{u_K} - A_{L,\sigma}(u) \textcolor{red}{u_L}$$

↑

$$\mu_{K,\sigma} \sum_{i=1}^{n_K} \alpha_{K,\sigma,i}$$

Step 2: construction of the final flux

$$\tilde{F}_{K,\sigma} = \left(\frac{|a_{K,\sigma}|}{|a_{K,\sigma}| + |a_{L,\sigma}|} \mu_{K,\sigma} \sum_{i=1}^{n_K} \alpha_{K,\sigma,i} \right) u_K - \left(\mu_{L,\sigma} a_{L,\sigma} - \mu_{K,\sigma} a_{K,\sigma} \right) u_L + B_\sigma$$

new NLTPFA[Gao & Wu, SISC'15]

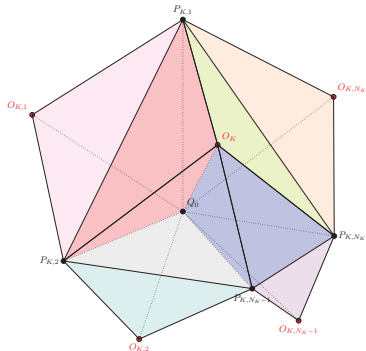
$$\tilde{F}_{K,\sigma} = A_{K,\sigma}(u) u_K - A_{L,\sigma}(u) u_L + B_\sigma^\epsilon$$

$\mu_{K,\sigma} \sum_{i=1}^{n_K} \alpha_{K,\sigma,i} + \frac{B_\sigma^+}{u_K + \epsilon}$

$\frac{B_\sigma^+ \epsilon}{u_K + \epsilon} - \frac{B_\sigma^- \epsilon}{u_L + \epsilon} \leq Ch^2$

Step 3: vertex interpolation algorithm¹

(1) The contour integrations of the normal component of flux along the boundaries of polyhedron $Q_0 O_k P_{k,1}, \dots, P_{k,N_k}$ is zero under linearity-preserving criterion.



We have the contour integration relation as follows

$$\sum_{k=1}^{N(Q_0)} \sum_{j=1}^{N_k} \mathbf{F}_k \cdot \mathbf{n}_0^{k,j} = 0.$$

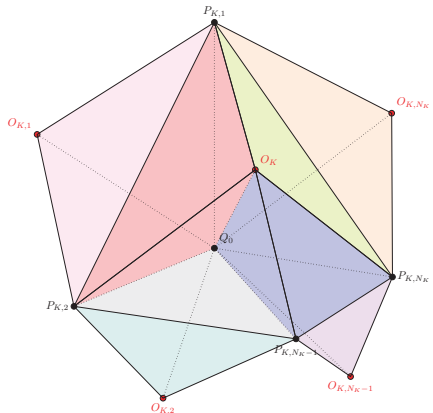
It can be known from the above discrete gradient that

$$\mathbf{F}_k \cdot \mathbf{n}_0^{k,j} = \zeta_{k,j,1}(u_{P_{k,j}} - u_0) + \zeta_{k,j,2}(u_{P_{k,j+1}} - u_0) + \zeta_{k,j,3}(u_k - u_0)$$

¹D. Yang, Z. Gao, G. Ni. IJNMF, 2022, 94(12): 2137-2171.

Step 3: vertex interpolation algorithm²

(2) We employ the flux continuity condition across the common face of the tetrahedron $O_k Q_0 P_{k,j} P_{k,j+1}$ and tetrahedron $O_{k,j} Q_0 P_{k,j} P_{k,j+1}$, i.e.



$$\mathbf{F}_k \cdot \mathbf{n}_f^{k,j} + \mathbf{F}_{k,j} \cdot (-\mathbf{n}_f^{k,j}) = 0.$$

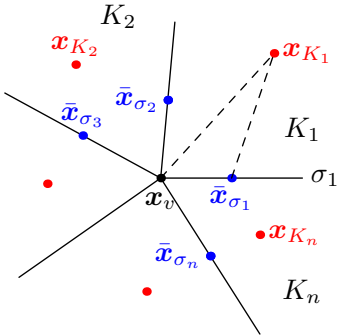
Thus, the explicit weight expression can be obtained

$$\omega_k = \frac{\psi_{k,1} + \sum_{m=1}^{\mathcal{N}(Q_0)} \sum_{i=2}^{N_m+1} \psi_{m,i} \cdot \delta(m, i, k)}{\sum_{k=1}^{\mathcal{N}(Q_0)} \left(\psi_{k,1} + \sum_{j=2}^{N_k+1} \psi_{k,j} \right)}.$$

²D. Yang, Z. Gao, G. Ni. IJNMF, 2022, 94(12): 2137-2171.

Step 3: vertex interpolation algorithm

2D version of vertex interpolation method can be found in [Gao, Wu, 2011]³



$$u_v = \sum_{i=1}^n w_i u_{K_i} \text{ with } w_i = \frac{\bar{w}_i}{\sum_{k=1}^n \bar{w}_k}$$

$$\begin{aligned}\bar{w}_k &= \frac{\eta_{k-1,1} - \eta_{k,2}}{\bar{\xi}_{k-1,2} + \bar{\xi}_{k,1}} \xi_{k,1} + \frac{\eta_{k,1} - \eta_{k+1,2}}{\bar{\xi}_{k,2} + \bar{\xi}_{k+1,1}} \xi_{k,2} \\ \xi_{i,j} &= \frac{1}{2S_{i,j}} (\mathcal{R}x_v \bar{x}_{\sigma_{i+j-1}})^T \Lambda_{K_i} \mathcal{R}(x_v \bar{x}_{\sigma_{i+j-1}}) \\ \bar{\xi}_{i,j} &= \frac{1}{2S_{i,j}} (\mathcal{R}(x_v \bar{x}_{\sigma_{i+j-1}}))^T \Lambda_{K_i} \mathcal{R}(x_{K_i} x_v) \\ \eta_{i,j} &= \frac{(\mathcal{R}(\bar{x}_{\sigma_i} \bar{x}_{\sigma_{i+1}}))^T \Lambda_{K_i} \mathcal{R}(x_v \bar{x}_{\sigma_{i+j-1}})}{2S_{\Delta x_v \bar{x}_{\sigma_i} \bar{x}_{\sigma_{i+1}}}}\end{aligned}$$

³Z. Gao, J. Wu. IJNMF, 67(12)(2011)2157-2183.

Step 4: the final finite volume equation

Finite volume equation

The PPFV scheme: find $\{u_K, K \in \mathcal{T}\}$ such that

$$\sum_{\sigma \in \mathcal{E}_K} \tilde{F}_{K,\sigma} = |K|f_K, \quad \forall K \in \mathcal{T}.$$

Now we get a nonlinear algebraic system $\mathbb{M}(\mathbf{U})\mathbf{U} = \mathbf{F}(\mathbf{U})$, which can be solved by Picard iterations.

Positivity of the discrete solution

Let $f \geq 0$, $g_D \geq 0$ and $g_N \leq 0$. Assume that $\sum_{i=1}^{n_K} \alpha_{K,\sigma,i} > 0$, $\forall \sigma \in \mathcal{T}$ holds. If the initial solution vector $\mathbf{U}^0 \geq 0$ and linear systems in the Picard iterations are solved exactly, then $\mathbf{U}^k \geq 0$ for $k \geq 1$.

Outline

- 1 Motivation
- 2 PPFV scheme for steady diffusion problem
- 3 PPFV scheme for three temperature model
- 4 Numerical examples

Three temperature radiation diffusion problems

The energy evolution of radiation, electrons and ions can be respectively described by

$$\begin{aligned}\frac{\partial E_e}{\partial t} - \nabla \cdot (\lambda'_e \nabla T_e) &= c\sigma_P (E_r - aT_e^4) + c\kappa (T_i - T_e) + Q_e, \\ \frac{\partial E_i}{\partial t} - \nabla \cdot (\lambda'_i \nabla T_i) &= c\kappa (T_e - T_i) + Q_i, \\ \frac{\partial E_r}{\partial t} - \nabla \cdot (\lambda_r \nabla E_r) &= c\sigma_P (aT_e^4 - E_r) + Q_r.\end{aligned}$$

- E_e, E_i and E_r are respectively the radiative, electronic and ionic energy densities.
- c denotes the speed of light, a denotes the Stefan constant;
- Planck opacity σ_P is a given nonlinear function of T_e and T_r ;
- κ is a positive relaxation coefficient which depends on T_e and T_i ;
- The electronic, ionic and radiative thermal conductivities are given by

$$\lambda'_\alpha = K_\alpha T_\alpha^{5/2}, \quad \alpha = e, i \quad (\text{Spitzer-Harm}) \quad \lambda_r = \frac{c}{3\sigma_R(T_e)} \quad (\text{Rosseland diffusion}).$$

Model recasting with $\phi_\alpha = aT_\alpha^4$

Following the idea in [Enaux, et.al., JSC2020]⁴, three temperature model is recast in the following form by setting $\phi_\alpha = aT_\alpha^4$:

$$\begin{aligned}\frac{\partial \phi_e}{\partial t} - \beta_e \nabla \cdot (\lambda_e \nabla \phi_e) &= \beta_e c \sigma_P (\phi_r - \phi_e) + \beta_e c \kappa \delta_{ie} (\phi_i - \phi_e) + \beta_e Q_e \\ \frac{\partial \phi_i}{\partial t} - \beta_i \nabla \cdot (\lambda_i \nabla \phi_i) &= \beta_i c \kappa \delta_{ie} (\phi_e - \phi_i) + \beta_i Q_i \\ \frac{\partial \phi_r}{\partial t} - \beta_r \nabla \cdot (\lambda_r \nabla \phi_r) &= \beta_r c \sigma_P (\phi_e - \phi_r) + \beta_r Q_r\end{aligned}$$

where

$$\lambda_e = \frac{\lambda'_e}{\rho c_{ve} \beta_e}, \quad \lambda_i = \frac{\lambda'_i}{\rho c_{vi} \beta_i}, \quad \lambda_r = \frac{c}{3\sigma_R}, \quad \beta_\alpha = \frac{d\phi_\alpha}{dE_\alpha} = \frac{d\phi_\alpha}{dT_\alpha} \frac{dT_\alpha}{dE_\alpha} = \frac{4aT_\alpha^3}{\rho c_{v,\alpha}}, \quad \alpha = e, i, r.$$

⁴C. Enaux, S.Guisset, C.Lasuen, Q.Ragueneau, J. Sci. Comput. (2020)82:51.

Spatial and temporal discretization of 3T model

The temporal discretization chosen consist in the backward-Euler scheme, and the spatial-temporal discretization of 3T model reads:

$$\phi_{e,K}^{n+1} - \phi_{e,K}^n + \frac{\tau}{|K|} \beta_{e,K}^{n+1} \sum_{\sigma \in \mathcal{E}_K} F_{e,K,\sigma}^{n+1} = \tau c \sigma_P \beta_{e,K}^{n+1} \left(\phi_{r,K}^{n+1} - \phi_{e,K}^{n+1} \right) + \tau \beta_{e,K}^{n+1} Q_{e,K}^{n+1}$$

$$+ \tau c \kappa \beta_{e,K}^{n+1} \delta_{ie,K}^{n+1} \left(\phi_{i,K}^{n+1} - \phi_{e,K}^{n+1} \right),$$

$$\phi_{i,K}^{n+1} - \phi_{i,K}^n + \frac{\tau}{|K|} \beta_{i,K}^{n+1} \sum_{\sigma \in \mathcal{E}_K} F_{i,K,\sigma}^{n+1} = \tau c \kappa \beta_i^{n+1} \delta_{ie,K}^{n+1} \left(\phi_{e,K}^{n+1} - \phi_{i,K}^{n+1} \right) + \tau \beta_{i,K}^{n+1} Q_{i,K}^{n+1},$$

$$\phi_{r,K}^{n+1} - \phi_{r,K}^n + \frac{\tau}{|K|} \beta_{r,K}^{n+1} \sum_{\sigma \in \mathcal{E}_K} F_{r,K,\sigma}^{n+1} = \tau c \sigma_P \left(\phi_{e,K}^{n+1} - \phi_{r,K}^{n+1} \right) + \tau \beta_{r,K}^{n+1} Q_{r,K}^{n+1},$$

where the derivation of face flux $F_{\alpha,K,\sigma}^{n+1}, \alpha = e, i, r$ is given in the previous section.

The final finite volume equation

The PPFV scheme for 3T model: find $\{u_K, K \in \mathcal{T}\}$ such that

$$\phi_{\alpha,K}^{n+1} + \sum_{\gamma \in \{e,i,r\}} w_{\alpha,\gamma,K}^{n+1} G_{\gamma,K}^{n+1} = \sum_{\gamma \in \{e,i,r\}} w_{\alpha,\gamma,K}^{n+1} \left(\phi_{\gamma,K}^n + q_{\gamma,K}^{n+1} \right), \quad \alpha = e, i, r, \forall K \in \mathcal{T}.$$

where

$$G_{\alpha,K}^{n+1} = \frac{\tau}{|K|} \beta_{\alpha,K}^{n+1} \sum_{\sigma \in \mathcal{E}_K} \tilde{F}_{\alpha,K,\sigma}^{n+1}, \quad q_{\alpha,K}^{n+1} = \tau \beta_{\alpha,K}^{n+1} Q_{\alpha,K}^{n+1},$$

and the definition of the flux

- For $\sigma \in \mathcal{E}_K \cap \mathcal{E}_L$: $\tilde{F}_{\alpha,K,\sigma}^n = A_{\alpha,K,\sigma}^n(\phi_\alpha^n) \phi_{\alpha,K}^n - A_{\alpha,L,\sigma}^n(\phi_\alpha^n) \phi_{\alpha,L}^n$
- For $\sigma \in \mathcal{E}_K \cap \Gamma_D$: $\tilde{F}_{\alpha,K,\sigma}^n = \lambda_{\alpha,K,\sigma}^n \sum_{i=1}^{N_{K,\sigma}} a_{K,\sigma,i} \left(\phi_{\alpha,K}^n - g_\alpha^D(\mathbf{x}_{K,\sigma,i}, t^n) \right), \quad \mathbf{x}_{K,\sigma,i} \in \sigma$
- For $\sigma \in \mathcal{E}_K \cap \Gamma_N$: $\tilde{F}_{\alpha,K,\sigma}^n = \int_{\sigma} g_\alpha^N(\mathbf{x}, t^n) \, ds$

The nonlinear algebraic system

We get a nonlinear algebraic system

$$\mathbb{M}(\phi^n)\phi^n = \mathbf{b}(\phi^n).$$

where

$$\mathbb{M}(\phi^n) = \tilde{\mathbb{M}}(\phi^n) + \mathbb{I},$$

and

$$\tilde{\mathbb{M}}(\phi^n) = \begin{bmatrix} \mathbb{W}_{e,e}^n \mathbb{A}_e^n & \mathbb{W}_{e,i}^n \mathbb{A}_i^n & \mathbb{W}_{e,r}^n \mathbb{A}_r^n \\ \mathbb{W}_{i,e}^n \mathbb{A}_e^n & \mathbb{W}_{i,i}^n \mathbb{A}_i^n & \mathbb{W}_{i,r}^n \mathbb{A}_r^n \\ \mathbb{W}_{r,e}^n \mathbb{A}_e^n & \mathbb{W}_{r,i}^n \mathbb{A}_i^n & \mathbb{W}_{r,r}^n \mathbb{A}_r^n \end{bmatrix}, \quad \phi^n = \begin{bmatrix} \phi_e^n \\ \phi_i^n \\ \phi_r^n \end{bmatrix}, \quad \mathbf{b}(\phi^n) = \begin{bmatrix} \tilde{\mathbf{b}}_e^n \\ \tilde{\mathbf{b}}_i^n \\ \tilde{\mathbf{b}}_r^n \end{bmatrix},$$

Some theoretical results

Positivity of the discrete solution

Let $\phi_\alpha^0 \geq 0$, $Q_\alpha \geq 0$, $g_\alpha^D \geq 0$, $g_\alpha^N \leq 0$, $\alpha \in \{e, i, r\}$, and assume that each mesh cell K is a star-shaped polyhedron w.r.t. x_K . If the initial solution vector $\phi^{n,0} \geq 0$ and linear systems in the Picard iterations are solved exactly, then $\phi^{n+1,k} \geq 0$ for $k \geq 1$.

Stability

Let $\phi_\alpha^0 \geq 0$, $Q_\alpha \geq 0$, $\alpha \in \{e, i, r\}$, assume that ($\Gamma = \partial\Omega$, $g_\alpha^D = 0$) and $\rho c_{v,\alpha} = 4a T_\alpha^3$, $\alpha = e, i$, then for $\phi_{\alpha,\mathcal{T}}^n = \{\phi_{\alpha,K}^n, K \in \mathcal{T}\} \in \mathbb{X}(\mathcal{T})$ we have

$$\left\| \phi_{\alpha,\mathcal{T}}^{N^t} \right\|_{L^1,\mathcal{T}} \leq \left(\left\| \phi_{m,\mathcal{T}}^0 \right\|_{L^1,\mathcal{T}} + \tau \sum_{k=1}^{N^t} \left\| Q_{m,\mathcal{T}}^k \right\|_{L^1,\mathcal{T}} \right), \quad \alpha = e, i, r.$$

where $\phi_{m,K}^n = \max_{\gamma \in \{e, i, r\}} \phi_{\gamma, K}^n$, $Q_{m,K}^n = \max_{\gamma \in \{e, i, r\}} Q_{\gamma, K}^n$, $t_{\max} = N^t \tau$.

Outline

- 1 Motivation
- 2 PPFV scheme for steady diffusion problem
- 3 PPFV scheme for three temperature model
- 4 Numerical examples

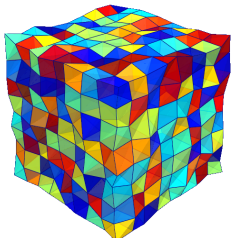
(P1) The continuous problem on nonplanar meshes

The computational domain $\Omega = [0, 1]^3$, and the diffusion tensor:

$$\Lambda = \begin{pmatrix} 1 & 0.5 & 0 \\ 0.5 & 1 & 0.5 \\ 0 & 0.5 & 1 \end{pmatrix}.$$

The exact solution:

$$u = 3 - (x^2 + y^2 + z^2), \quad (x, y, z) \in \Omega.$$

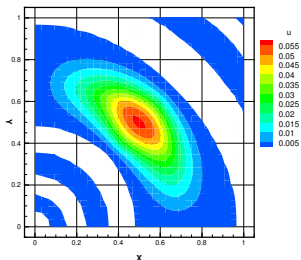


nunkw	E_u	R_u	E_q	R_q	umin	umax
64	1.05E-02	-	6.18E-02	-	3.870E-01	2.888
512	2.45E-03	2.095	2.33E-02	1.405	2.447E-01	2.972
4096	5.83E-04	2.069	9.24E-03	1.336	1.061E-01	2.993
32768	1.43E-04	2.027	4.05E-03	1.190	5.602E-02	2.998

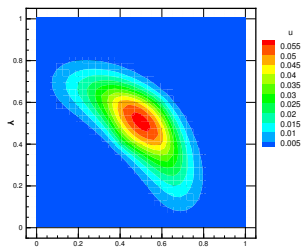
(P2) Positivity of the solution

The anisotropic diffusion tensor and the source term:

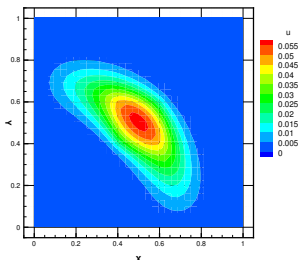
$$\Lambda = \begin{pmatrix} y^2 + cx^2 & -(1-c)xy & 0 \\ -(1-c)xy & x^2 + cy^2 & 0 \\ 0 & 0 & 1 \end{pmatrix}, \quad f = \begin{cases} 1, & (x, y) \in \left[\frac{3}{8}, \frac{5}{8}\right]^2, \ z \in [0, 1], \\ 0, & \text{otherwise,} \end{cases}$$



Linear LPFV



PPFV_LPDI



PPFV_LPDII

(P3) Convergence test for a continuous 3T model



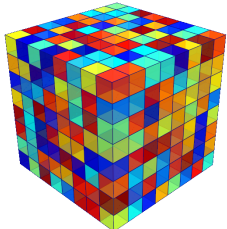
We set the computational domain $\Omega = [0, 1]^3$, and the following exact solution

$$\phi_e = 1 - 2(x - 0.5)^2 - (y - 0.5)^2 - (z - 0.5)^2,$$

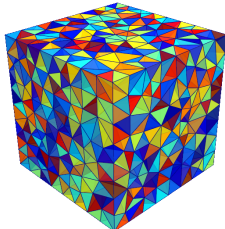
$$\phi_i = 1 - (x - 0.5)^2 - 2(y - 0.5)^2 - (z - 0.5)^2,$$

$$\phi_r = 1 - (x - 0.5)^2 - (y - 0.5)^2 - 2(z - 0.5)^2,$$

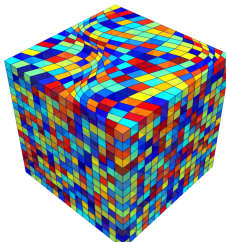
The associated parameter: $\rho c_{v,\alpha} = 4a T_\alpha^3$, $a = c = \sigma_P = \sigma_R = 1$, $\lambda_e = 1$, $\lambda_i = 0.5$.



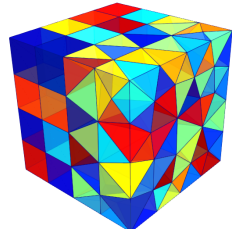
(a) Mesh1



(b) Mesh2

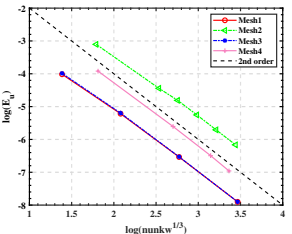
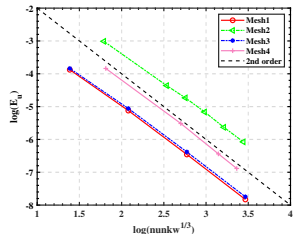
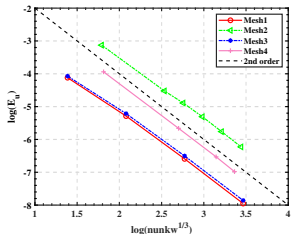


(c) Mesh3

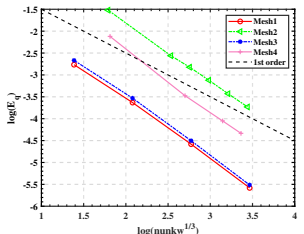
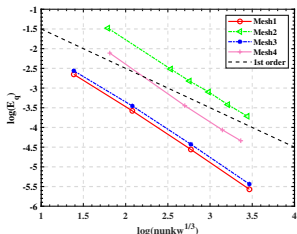
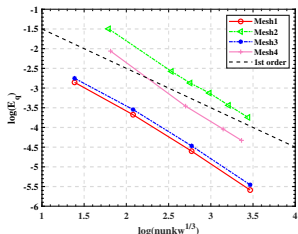


(d) Mesh4

(P3) Convergence test for a continuous 3T model



L^2 error of electronic (left), ionic (middle) and radiative (right) energy densities.



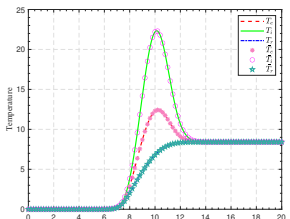
H^1 error of electronic (left), ionic (middle) and radiative (right) energy densities.

(P4) OD test (no spatial variation)

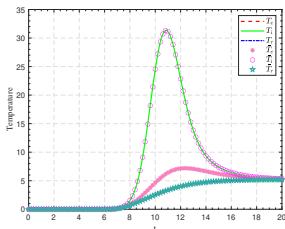
- **Problem 1–Problem 2:** At initial time the three temperatures are equal.
- A decoupling of the three temperatures are observed when source terms Q are applied:

$$Q_i(t) = \frac{A}{\sqrt{2\pi t_w}} \exp\left(-\left(\frac{t-t_c}{\sqrt{2t_w}}\right)^2\right), \quad Q_e = Q_r = 0.$$

	Problem 1	Problem 2
c	29.979	29.979
a	0.01372	0.01372
σ_P	$0.5 T_e^{-2}$	$0.1 T_e^{-2}$
κ	0.1	$0.01379 T_e^{-0.5}$
$\rho c_{v,i}$	0.15	0.15
$\rho c_{v,e}$	0.3	$0.3 T_e$
T_α	$2.52487 \cdot 10^{-5}$	$2.52487 \cdot 10^{-5}$
A	75.19884	15.03978



Problem 1



Problem 2

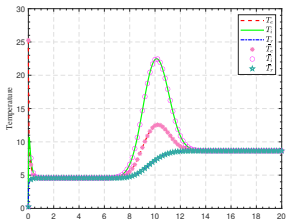
The numerical results in [1]¹ are recovered.
The ionic temperature is higher than others.

¹[1]C. Enaux, et.al., J. Sci. Comput. (2020)82:51.

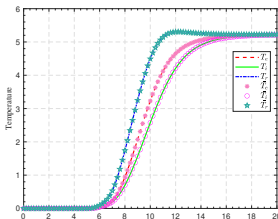
(P4) OD test (no spatial variation)

- **Problem 3:** source term is applied on ions, and the initial temperatures are different.
- **Problem 4:** source term is applied on photons.

	Problem 3	Problem 4
c	29.979	29.979
a	0.01372	0.01372
σ_P	$0.5 T_e^{-2}$	$0.1 T_e^{-2}$
κ	0.1	$0.01379 T_e^{-0.5}$
$\rho c_{v,i}$	0.15	0.15
$\rho c_{v,e}$	0.3	$0.3 T_e$
T_e	$2.52487 \cdot 10^{-1}$	$2.52487 \cdot 10^{-5}$
T_i	$2.52487 \cdot 10^1$	$2.52487 \cdot 10^{-5}$
T_r	$2.52487 \cdot 10^{-1}$	$2.52487 \cdot 10^{-5}$
A	75.19884	15.03978



Problem 3



Problem 4

The time evolution of temperatures are graphically shown, and the numerical results in [1]¹ are exactly recovered.

¹[1]C. Enaux, et.al., J. Sci. Comput. (2020)82:51.

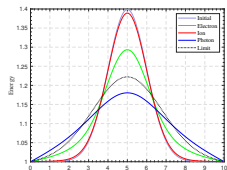
(P5) Asymptotic behavior

The asymptotic-preserving property is studied: $T_e = T_i = T_r$ when $c\sigma_P \rightarrow \infty$ and $c\kappa \rightarrow \infty$.

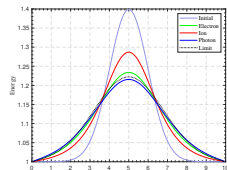
- Choose an initial energy profile for different values of $c\sigma_P$ and $c\kappa$ of the form

$$\phi_e = \phi_i = \phi_r = 1 + \frac{1}{\sqrt{2\pi}} \exp(-0.5(x-5)^2).$$

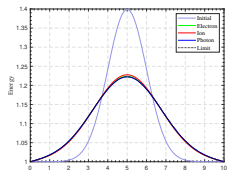
- For small values of $c\sigma_P$, the three temperature profiles are very different while they become closer as $c\sigma_P$ and $c\kappa$ increases.
- For large values $c\sigma_P = c\kappa$, it is expected that **the three temperatures to be equal**.



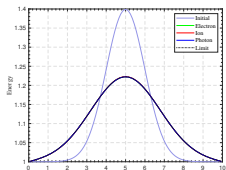
$$c\sigma_P = c\kappa = 10^{-1}$$



$$c\sigma_P = c\kappa = 10^0$$



$$c\sigma_P = c\kappa = 10^1$$

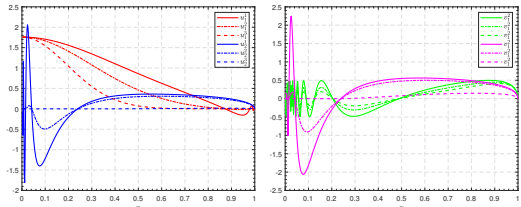
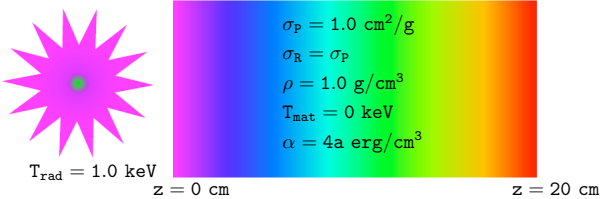


$$c\sigma_P = c\kappa = 10^2$$

(P6) The Su–Olson problem

- The Su-Olson problem⁵ consists of a half-space, non-equilibrium Marshak wave.
- As the energy density of the radiation field increases, energy is transferred to the material.
- The dimensionless solution for the radiation energy density:

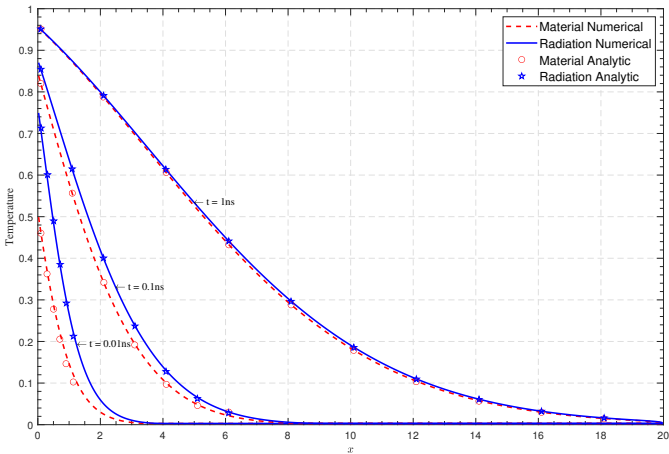
$$u(x, \tau, \epsilon) = 1 - \frac{2\sqrt{3}}{\pi} \int_0^1 \left[\frac{\sin[x\gamma_1(\eta, \epsilon) + \theta_1(\eta)]}{\eta \sqrt{3+4\gamma_1^2(\eta, \epsilon)}} \right] e^{-\tau\eta^2} d\eta - \frac{\sqrt{3}e^{-\tau}}{\pi} \int_0^1 \left[\frac{\sin[x\gamma_2(\eta, \epsilon) + \theta_2(\eta)]}{\eta(1+\epsilon\eta) \sqrt{3+4\gamma_2^2(\eta, \epsilon)}} \right] e^{\frac{-\tau}{\epsilon}\eta} d\eta.$$



Setup and parameters for the Su-Olson problem, and key components of the solution.

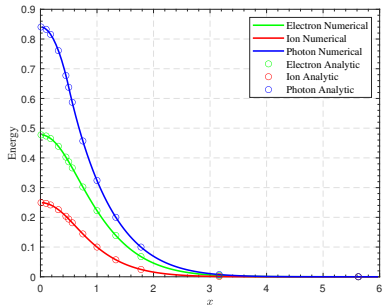
⁵B.Su,G.L.Olson, JQSRT, 1996, 56 (3): 337–351

(P6) The Su–Olson problem

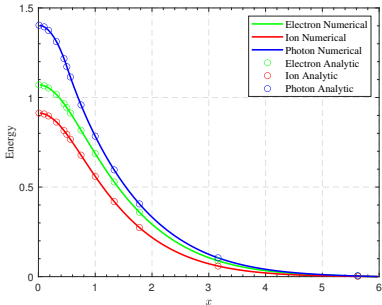


- Initially, the radiation streams into the slab and T_m lags behind T_r ;
- As the radiation energy density builds up, the material temperature catches up;
- At $t = 1\text{ns}$, the radiation and material temperatures are essentially identical.

(P7) A 3T version of the Su–Olson problem ⁷



(e) $t_m = 3.16228$



(f) $t_m = 10$

- A 3T version of the fixed-source problem solved by Su–Olson ⁶ which is useful for verifying computer code such as xRage code.
- An excellent agreement between the numerical and semi-analytical solutions can be seen.

⁶B.Su, G.L.Olson, Ann.Nucl.Energy,1997;24(13):1035–55

⁷R.G.McClarren, J.G.Wohlbier. JQSRT, 2011;112(1):119–130.

Summary

- Presented nonlinear two-point flux discretization for three temperature model
- Local mass conservation
- Positivity-preserving property
- Arbitrary polyhedral meshes
- SPD diffusion matrix for three temperature model
- Second-order convergence rate for temperature
- First-order convergence rate for flux
- Stability result for the discrete FV equations
- Coupling with Lagrangian hydrodynamics is easy

Key References

- D. Yang, Z. Gao, G. Ni. The positivity-preserving finite volume scheme with fixed stencils for anisotropic diffusion problems on general polyhedral meshes. International Journal for Numerical Methods in Fluids, 2022, 94(12): 2137-2171.
- G. Peng, Z. Gao, W. Yan, X. Feng. A positivity-preserving finite volume scheme for three-temperature radiation diffusion equations. Applied Numerical Mathematics, 2020, 152:125-140.
- Z. Gao, J. Wu. A second-order positivity-preserving finite volume scheme for diffusion equations on general meshes. SIAM J. Sci. Comput., 37(1)(2015)A420-A438
- J. Wu, Z. Gao. Interpolation-based second-order monotone finite volume schemes for anisotropic diffusion equations on general grids. Journal of Computational Physics 275 (2014) 569-588.
- Z. Gao, J. Wu. A linearity preserving cell-centered scheme for the heterogeneous and anisotropic diffusion equations on general meshes. Int. J. Numer. Meth. Fluids, 67(12)(2011)2157-2183.

铸国防基石，
做民族脊梁！

Thank you!

